International Conference in Recent Trends in Information Technology and Computer Science (ICRTITCS - 2012)
Proceedings published in International Journal of Computer Applications® (IJCA) (0975 – 8887)

Computational Modeling of Nanoscale Droplet Deposition Phenomena

Salil Desai
Department of Industrial & Systems Engineering
North Carolina A&T State University
Greensboro, NC 27411, USA

Ravindra Kaware
Department of Industrial & Systems Engineering
North Carolina A&T State University
Greensboro, NC 27411, USA

ABSTRACT
This research investigates nanoscale droplet deposition phenomena towards developing nanomanufacturing processes. The deposition and spreading behavior of water nanodroplet on SiO_2 and Si_3N_4 substrates is studied using molecular dynamics simulation. The effect of temperature variations on the dynamic contact angle during the wetting phenomena is observed. SiO_2 and Si_3N_4 substrates reveal a hydrophilic and hydrophobic interaction with water, respectively. An experimental design is conducted to observe the effect of substrate type and temperature on the time to reach equilibrium contact angle. Both factors and their interaction have a statistical significant effect on the equilibration time. The results of this research form a basis to predict wetting behavior for aqueous colloids on different substrates towards nanoscale manufacturing.

Keywords
Computational modeling, nanotechnology, nanodroplet, nanomanufacturing, statistical analysis, substrate deposition.

1. INTRODUCTION
Nanoscale manufacturing deals with fabrication of structures and features with dimensions of the order of 100nm or less [1]. In order to accomplish this goal several nanomanufacturing processes are being developed that employ nanoscale liquids that interact with substrates. Thus, it is important that the underlying physical phenomena be understood and explored to aid optimization of process parameters.

Direct-write processes such as dip-pen lithography, electrospraying and inkjet based methods deposit liquid droplets at varying length scales. These processes have recently been applied to biological fields such as tissue engineering [2] and drug delivery [3]. The high-resolution direct printing technique is of particular interest as a substitute to conventional vacuum deposition and photolithographic patterning of functional films such as gate electrodes, gate dielectrics, source and drain contacts and active semiconductor layers [4].

In the present research we investigate the deposition of water nanodroplet on substrates that are primary candidates for different applications including photonics, semiconductor electronics, bio-sensors, etc. [5]. Water plays a significant role as a universal solvent and is used as a fluid carrier for nanomaterials. The interaction of aqueous colloids with substrate materials has been well studied at the macro and micro scales [6]. However, nanoscale liquid-substrate interaction is an evolving body of research that entails further investigation.

2. BACKGROUND REVIEW
The interaction between nanoscale liquid with different substrate materials such as graphite [7], polymers [8], metals [9] and self-assembled monolayers [10] has been reported. Similarly, on the biological side, the effect of surface tension on contact angles between a protein solution and substrate made from silicon compounds has been studied [11]. In addition, substrate materials have been mimicked using range of solid surface energies to predict wetting behavior [12]. Further, the water nanodroplet model has been extensively studied in literature. However, the interaction of water nanodroplet with substrate materials at elevated temperatures is of interest for the nanomanufacturing processes being considered in this research. Further, understanding the interplay between temperature and substrate type can enable the optimization of process parameters.

3. METHODOLOGY
The nanoscale droplet deposition phenomenon was modeled using the Nanoscale Molecular Dynamics (NAMD) source code. Visual Molecular Dynamics (VMD) graphics was used for preprocessing the molecular model and graphics analysis of simulation results. NAMD and VMD were developed by the Theoretical and Computational Biophysics Group in the Beckman Institute for Advanced Science and Technology at the University of Illinois at Urbana-Champaign [13]. NAMD source code has been benchmarked for computational robustness over other MD codes for the molecular system being analyzed in this research. In addition, it is compatible with a wide range of force fields from the CHARMM and AMBER systems. In this paper, we study the interaction of water nanodroplet with two substrate types. An integrated model was developed that included a water nanodroplet encapsulated within vapor ambience (water box) which was further placed on the substrate interface.

3.1 Molecular model of water
The water nanodroplet was built using the modified TIP3P water molecular model adopted within the CHARMM force field system. A 4 nm diameter nanodroplet model was built using 3,171 water atoms (1,057 molecules). Further, the water nanodroplet was enclosed in cubical water box with sides of

4.65 nm using 5,361 water atoms (1,787 molecules). The water box simulated vapor ambience to track transient drop evaporation and spreading. Periodic boundary conditions were enforced for the simulation control volume. Figure 1 shows the molecular model of the water nanodroplet encapsulated within the water box.

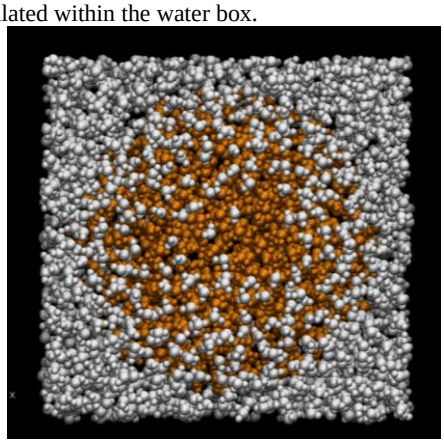

Fig 1: Molecular model of water nanodroplet encapsulated within the water box

A SiO_2 substrate model was built using 42,336 SiO_2 atoms (20.8 nm X 20.8 nm X 3.37 nm). Similarly, a Si_3N_4 substrate model was built using 11,718 Si_3N_4 atoms (32.03 nm X 26.21 nm X 2.42). A water nanodroplet was placed at the interface of SiO_2 and Si_3N_4 substrates, as shown in Fig. 2 and Fig. 3, respectively.

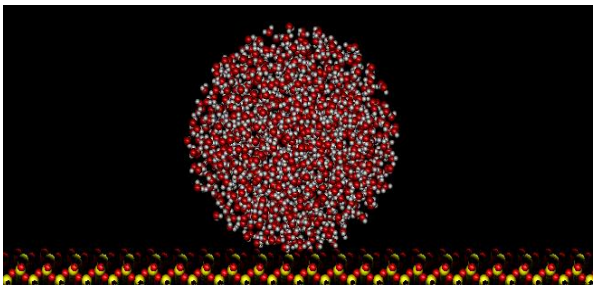

Fig 2: Water nanodroplet placed on SiO_2 substrate

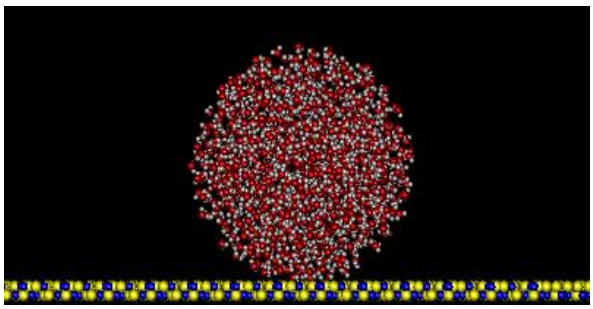

Fig 3: Water nanodroplet placed on Si_3N_4 substrate

3.2 Solution scheme

The Particle Mesh Ewald (PME) method was used to resolve temperature, pressure, and electrostatic forces. The smooth PME method was used for full electrostatic computations. The potential energy function used for the MD simulations can be simplified as:

$$U_{Total} = U_{Bond} + U_{Angle} + U_{Dihedral} + U_{vdW} + U_{Coulomb} \quad (1)$$

Where, U_{Bond}, U_{Angle}, and $U_{Dihedral}$ denote the stretching, bending and torsional bonding interactions, respectively. U_{vdW} and $U_{Coulomb}$ account for interactions between nonbonded atom pairs that correspond to the van der Waal's forces; predicted by a Lennard-Jones 6-12 potential and the electrostatic interactions, respectively. Validated force field parameters from CHARMM were used to determine the extent of the bonding interactions. The inter-molecular interaction among water molecules was described by pair-wise additive Lennard-Jones potential as described in equation 2.

$$E_{LJ} = 4\varepsilon\left[\left(\frac{\sigma}{r_{ij}}\right)^{12} - \left(\frac{\sigma}{r_{ij}}\right)^{6}\right] \quad (2)$$

where, E_{LJ} is the intermolecular potential between the two atoms or molecules, ε is a measure of attraction between two particles, and σ is the distance at which the intermolecular potential between the two particles becomes zero. The center-to center distance between two particles is denoted by r_{ij}.
To avoid surface effects at the boundary of the simulated system, a periodic boundary condition was used where the particles confined in a simulation cell were mimicked in the space through periodic translations of particles. This scheme ensures that there is always a vapor environment that envelopes spreading droplet. An NPT ensemble (constant temperature, pressure, number of particles and variable volume) was used for all simulations.

The SiO_2-water and Si_3N_4-water models were simulated at 293 K, 323 K, 373 K and 473 K with a 0.5 femtosecond time step. The temperature was held constant by Langevin dynamics. Similarly, the pressure was maintained (NPT ensemble simulations) by Nosé-Hoover-Langevin piston at 1 bar. Lennard-Jones switching function of 12 Å and PME grid size of 1 were adopted for all simulations. Multiple time step integration was accomplished using impulse-based Verlet-I/r-RESPA method.

4. RESULTS AND DISCUSSION

The SiO_2-water system was simulated for a period of 100 picosecond (ps) and the Si_3N_4-water system was simulated for 1 nanosecond (ns), respectively. The spreading behavior for both the systems was observed at different temperatures (293 K, 323 K, and 373 K). The SiO_2-water system was simulated for shorter period due to hydrophilic nature of SiO_2 substrate which expedites spreading phenomenon and the equilibrium contact angle can be observed well within the 100 ps time period. However, Si_3N_4-water system was simulated up to 1 ns because of hydrophobic behavior of Si_3N_4 substrate that causes delay in reaching equilibrium. The dynamic contact angles were measured using Image-J software (NIH). Simulation images at chosen time intervals were analyzed in Image-J software and the average contact angles for both the systems were determined as shown in Fig. 4.

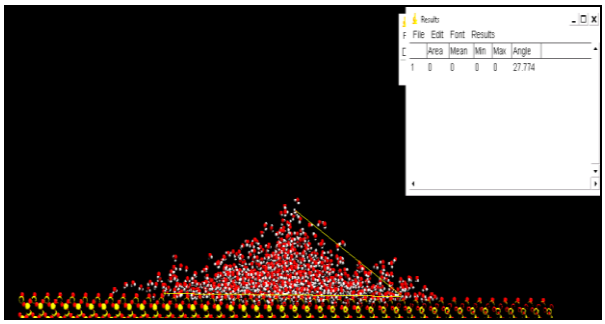

Fig 4: Dynamic contact angle measurement in Image-J

4.1 Comparison of Progressive Spreading

Figure 5 shows the progression of nanodroplet spreading phenomena on SiO_2 and Si_3N_4 substrates at 293 K, respectively. The water nanodroplet spreads rapidly on SiO_2 substrate revealing the hydrophilic interaction by attaining an equilibrium contact angle of (27^o) within 70 ps. However, nanodroplet shows hydrophobic interaction with Si_3N_4 substrate and takes 410 ps to reach equilibrium contact angle (42^o). Thus, indicating a delayed wetting behavior (time to reach equilibrium in Si_3N_4 is approximately six times longer as compared to SiO_2-water system).

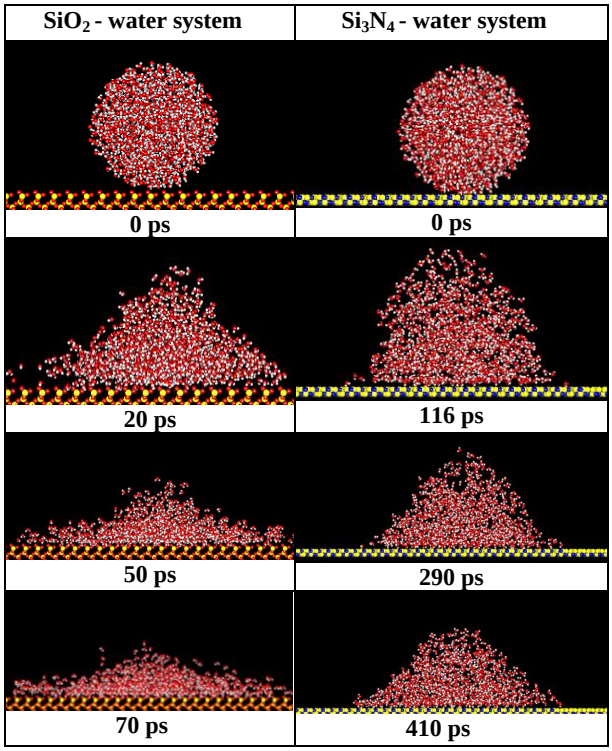

Fig 5: Comparison of progressive nanodroplet spreading on substrates

4.2 Dynamic Contact Angle for SiO_2-water system

The dynamic contact angles for the SiO_2-water system was evaluated for different temperatures as shown in Fig. 6 through 9. An equilibrium contact angle of 27.5^o confirms strong hydrophilic behavior of SiO_2 substrate while interacting with water nanodroplet and closely follows macroscale SiO_2-water wetting characteristics.

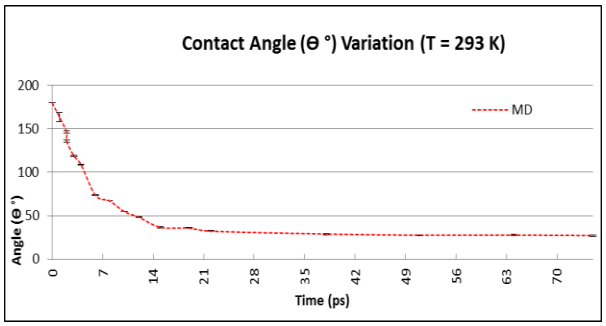

Fig 6: Dynamic contact angle for SiO_2-water system (T = 293K)

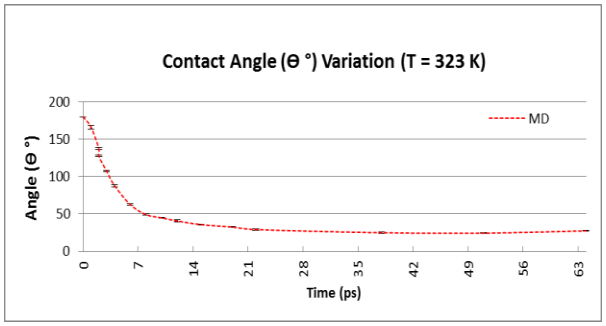

Fig 7: Dynamic contact angle for SiO_2-water system (T = 323 K)

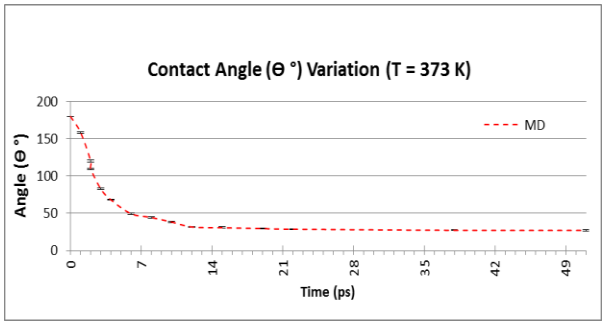

Fig 8: Dynamic contact angle for SiO_2-water system (T = 373 K)

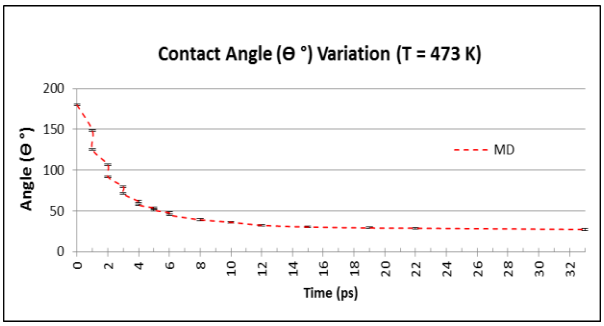

Fig 9: Dynamic contact angle for SiO_2-water system (T = 473 K)

At higher temperatures the equilibrium contact angle was attained earlier as compared to lower temperatures. This is

due to the increase in surface energy of the substrate which entails faster spreading rates. Thus, the equilibrium contact angle at 293 K was reached at around 70 ps whereas for 473 K, equilibrium contact angle was observed approximately at 35 ps. Similarly, the equilibrium contact angle for 323 K and 373 K were attained at intermediate time periods of 65 ps and 52 ps, respectively.

4.3 Dynamic Contact Angle for Si_3N_4-water system

The dynamic contact angles for the Si_3N_4-water system evaluated at different temperatures are shown in Fig. 10 through 13.

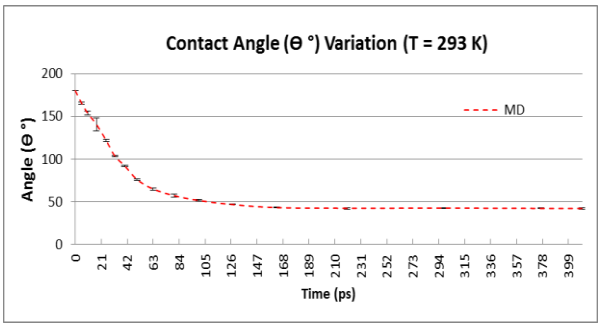

Fig 10: Dynamic contact angle for Si_3N_4-water system (T = 293 K)

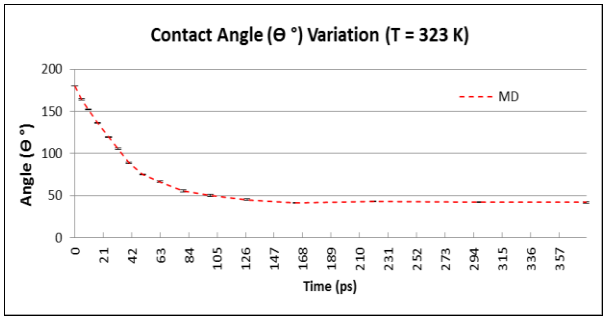

Fig 11: Dynamic contact angle for Si_3N_4-water system (T = 323 K)

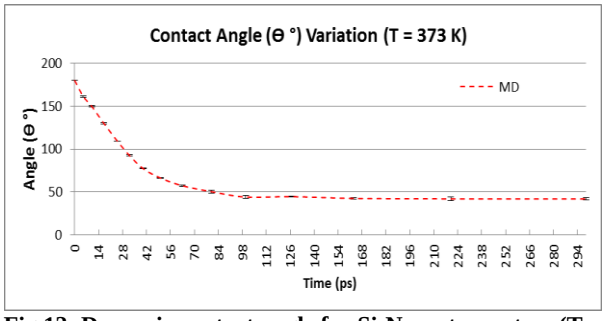

Fig 12: Dynamic contact angle for Si_3N_4-water system (T = 373 K)

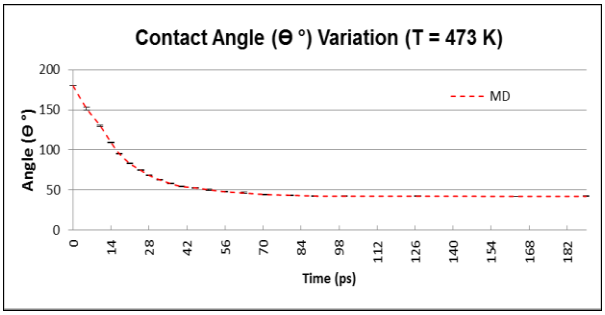

Fig 13: Dynamic contact angle for Si_3N_4-water system (T = 473 K)

For the Si_3N_4-water system, the equilibrium contact angle was observed at approximately 42.08° which was in close agreement with macroscale Si_3N_4-water equilibrium contact angle. However, the spreading time was substantially higher at all temperatures compared to the SiO_2-water system at corresponding temperatures. At 293 K the Si_3N_4-water system attained the equilibrium contact angle at 410 ps as compared to 192 ps for 473 K. Similarly, the equilibrium contact angle for 323 K and 373 K were attained at intermediate time periods of 377 ps and 301 ps, respectively. Furthermore, this difference in spreading mechanism between Si_3N_4-water system and SiO_2-water system was consistently evident at all temperatures.

4.4 Design of Experiments

An experimental design was conducted to study the effect of two factors namely; (1) temperature and (2) substrate type on the time to reach equilibrium contact angle. The multilevel factorial design is shown in Table 1. Two replicates were obtained from simulation runs as an estimate for error. The data sets were validated for randomness and normality assumptions.

Table 1. Multilevel factorial design

Factors	Level	Values
Temperature	4	293, 323, 373, 473
Substrate Type	2	SiO_2, Si_3N_4

Figure 14 shows the main effects of temperature and substrate on the time to reach equilibrium contact angle. The data sets were validated for randomness and normality assumptions. Table 2. shows the Analysis of Variance (ANOVA) for the equilibrium time. From the ANOVA results, it is evident that temperature, substrate type and their interaction have statistically significant effect on the equilibrium time based on a p-value of 0.000. Also, the high R-Sq value confirms a goodness of fit for the data set.

Table 2. ANOVA for equilibrium time

Source	DF	SeqSS	AdjSS	AdjMS	F	P
Temp	3	40831	40831	13610	3738.48	0.0
Subst	1	240958	240958	240958	66185.96	0.0
Temp x Subst	3	20874	20874	6958	1911.21	0.0
Error	8	29	29	4		
Total	15	302693				
S = 1.90804, R-Sq = 99.99%, R-Sq(adj) = 99.98%						

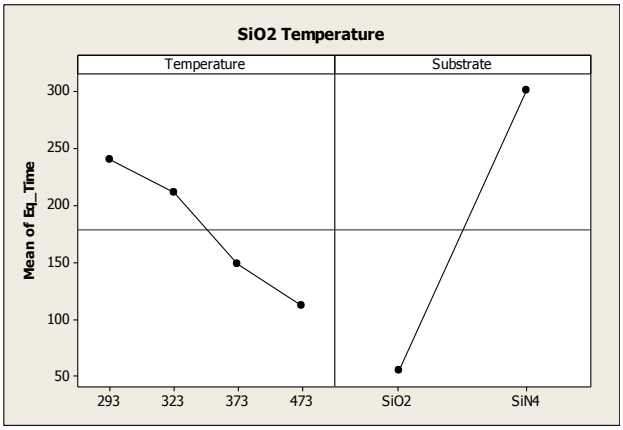

Fig 14: Main effects for temperature and substrate type

Figure 14 show that substrate type has a profound effect on the equilibrium time as compared to temperature variations. This can be attributed to the hydrophobic nature of Si_3N_4 which retards the spread and prolongs the equilibrium time. However, both main factors have a statistically significant effect on equilibrium time as indicated by ANOVA results.

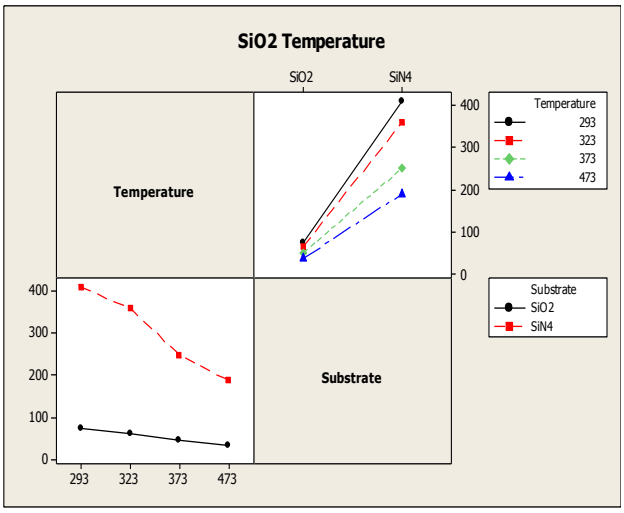

Fig 15: Interaction effects for temperature and substrate type

Figure 15 shows interaction effects of temperature and substrate type factors on equilibrium time. For the Si_3N_4 substrate the equilibrium time drops rapidly at higher temperatures as compared to SiO_2 substrate. This is due to the increase in surface energy of the substrate at higher temperatures that facilitates faster spreading of the water molecules. Further, the interaction effects were sliced with respect to both temperature and substrate type to identify statistical significance.

5. CONCLUSIONS

This paper describes the spreading behavior of water nanodroplet on SiO_2 and Si_3N_4 substrates at different temperatures. The water nanodroplet-SiO_2 substrate interaction revealed a hydrophilic spreading and yielded an equilibrium contact angle of 27.5^o. At higher temperatures, the time to reach equilibrium contact angle was shorter due to lowering of the surface tension of the liquid nanodroplet and increase in the surface energy of the substrates.

The water nanodroplet-Si_3N_4 substrate interaction displayed a hydrophobic behavior at nanoscale (identical with macroscale behavior) at all four temperatures. Hydrophobic nature of interaction was characterized by higher equilibrium contact angle of 42.08^o compared to 27.5^o for hydrophilic SiO_2-water system. In contrast to the SiO_2-water system, the equilibrium contact angle for Si_3N_4-water system was attained at longer time periods. Based on a design of experiments, both the factors (1) substrate type and (2) temperature had statistically significant influence on the spreading dynamics of the nanoscale deposition phenomenon. The effect of substrate type was profound as compared to temperature variations on the equilibrium time. The results from this research provide a foundation to develop relationships between temperature gradients and substrate type for wetting characteristics. These findings are vital for nanoscale manufacturing using a variety of nanocolloids in combination with different substrates.

6. ACKNOWLDGEMENTS

The authors extend their gratitude to the US National Science Foundation (NSF CMMI: Award 0846562) for support towards this research.

7. REFERENCES

[1] Xia, Y., Rogers, J. A., Paul, K. E., and Whitesides, G. M. 1999. Unconventional methods for fabricating and patterning nanostructures. Chemical Reviews-Columbus. 99(7), 1823-1848.

[2] Sachlos, E., and Czernuszka, J. 2003. Making tissue engineering scaffolds work. Review: the application of solid freeform fabrication technology to the production of tissue engineering scaffolds. Eur. Cell Mater. 5(29), 39-40.

[3] Hon, K., Li, L., and Hutchings, I. M. 2008. Direct writing technology--Advances and developments. CIRP Annals-Manufacturing Technology. 57(2), 601-620.

[4] Zschieschang, U., Klauk, H., Wadepohl, H., and Klauk, L. H. 2003. Flexible organic circuits with printed gate electrodes. Advanced Materials. 15(14), 1147-1151.

[5] Pique, A., and Chrisey, D. B. 2002. Direct-write technologies for rapid prototyping applications: sensors, electronics, and integrated power sources. Academic Press.

[6] Kropman, M. F., and Bakker, H. J. 2001. Dynamics of water molecules in aqueous solvation shells. Science. 291(5511), 2118-2120.

[7] Werder, T., Walther, J. H., Jaffe, R. L., Halicioglu, T., and Koumoutsakos, P. 2003. On the water-carbon interaction for use in molecular dynamics simulations of graphite and carbon nanotubes. The Journal of Physical Chemistry B. 107(6), 1345-1352.

[8] Hirvi, J. T., and Pakkanen, T. A. 2006. Molecular dynamics simulations of water droplets on polymer surfaces. The Journal of Chemical Physics. 125(14), 144712.

[9] Shibuta, Y., and Suzuki, T. 2010. Phase transition in substrate-supported molybdenum nanoparticles: a molecular dynamics study. Phys. Chem. Chem. Phys. 12(3), 731-739.

[10] Park, S. H., Carignano, M. A., Nap, R. J., and Szleifer, I. 2010. Hydrophobic-induced surface reorganization: molecular dynamics simulations of water nanodroplets on perfluorocarbon self-assembled monolayers. Soft Matter. 6(8), 1644-1654.

[11] Tseng, F. G., Huang, C. Y., Chieng, C. C., Huang, H., and Liu, C. S. 2002. Size effect on surface tension and contact angle between protein solution and silicon compound, PC, and PMMA substrates. Microscale Thermophysical Engineering. 6(1), 31-53.

[12] Hong, S. D., Ha, M. Y., and Balachandar, S. 2009. Static and dynamic contact angles of water droplet on a solid surface using molecular dynamics simulation. Journal of Colloid and Interface Science. 339(1), 187-195.

[13] Nelson, M., Humphrey, W., Gursoy, A., Dalke, A., Kalé, L., Skeel, R. D., and Schulten, K. 1996. NAMD: a parallel, object-oriented molecular dynamics program. International Journal of High Performance Computing Applications. 10(4), 251-268.